Materials Horizons

ROYAL SOCIETY OF CHEMISTRY

MINIREVIEW

View Article Online
View Journal | View Issue

Cite this: *Mater. Horiz.*, 2021, **8**, 3266

Gels as emerging anti-icing materials: a mini review

Yizhi Zhuo, [a] Jianhua Chen, [b] Senbo Xiao, [a] Tong Li, [a] Feng Wang, [a] Jianying He *[a] and Zhiliang Zhang *[a]

Gel materials have drawn great attention recently in the anti-icing research community due to their remarkable potential for reducing ice adhesion, inhibiting ice nucleation, and restricting ice propagation. Although the current anti-icing gels are in their infancy and far from practical applications due to poor durability, their outstanding prospect of icephobicity has already shed light on a new group of emerging anti-icing materials. There is a need for a timely review to consolidate the new trends and foster the development towards dedicated applications. Starting from the stage of icing, we first survey the relevant anti-icing strategies. The latest anti-icing gels are then categorized by their liquid phases into organogels, hydrogels, and ionogels. At the same time, the current research focuses, anti-icing mechanisms and shortcomings affiliated with each category are carefully analysed. Based upon the reported state-of-the-art anti-icing research and our own experience in polymer-based anti-icing materials, suggestions for the future development of the anti-icing gels are presented, including pathways to enhance durability, the need to build up the missing fundamentals, and the possibility to enable stimuli-responsive properties. The primary aim of this review is to motivate researchers in both the anti-icing and gel research communities to perform a synchronized effort to rapidly advance the understanding and making of gel-based next generation anti-icing materials.

Received 9th June 2021,
Accepted 16th August 2021

DOI: 10.1039/d1mh00910a

rsc.li/materials-horizons

[a] *NTNU Nanomechanical Lab, Department of Structural Engineering, Norwegian University of Science and Technology (NTNU), Trondheim 7491, Norway. E-mail: jianying.he@ntnu.no, zhiliang.zhang@ntnu.no*

[b] *College of Chemistry, Chemical Engineering and Environment, Minnan Normal University, Zhangzhou 363000, China*

Yizhi Zhuo

Yizhi Zhuo completed his bachelor's degree in applied chemistry at South China University of Technology in 2013, and then master's degree in chemical engineering at Xiamen University in 2016. In 2019, he received his PhD degree from Norwegian University of Science and Technology (NTNU), where he worked on designing durable icephobic materials. He is currently working as a postdoctoral fellow at NTNU Nanomechanical Lab. His research focuses on designing and synthesizing polymeric materials for anti-icing and exploring the underlying mechanisms.

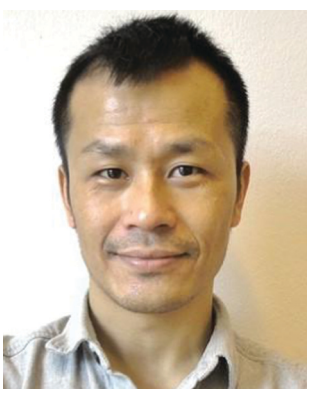

Senbo Xiao

Senbo Xiao studied physics at Nankai University, China, and biophysics at Heidelberg University, Germany. After receiving his PhD degree in 2011, he worked in the Heidelberg Institute for Theoretical Studies and the Max Planck Institute for Polymer Research as a postdoctoral fellow focusing on materials mechanics of polymers and polymer nanocomposites. He is now a researcher in the Norwegian University of Science and Technology (NTNU) Nanomechanical Lab concentrating on surface phenomena and interface mechanics. His current research interests include design and applications of nanomaterials for purposes of anti-icing and enhanced-oil recovery.

Introduction

Unwanted icing has always been a severe challenge to human activities. Frozen water on exposed surfaces of aircrafts, ships, windmills, and power lines can cause high energy consumption and even catastrophic accidents.[1–3] To ameliorate the detrimental effects of icing, traditional active de-icing methods by using chemicals, heat, and mechanical force have been adopted.[4,5] For example, anti-freezing liquids are sprayed on the fuselage to avoid the freezing of water. Salts are spilled on roads to reduce traffic accidents. Mechanical de-icing of transmission lines is usually applied to prevent collapse and safety problems. However, these traditional methods to remove the accreted ice require periodic operations, high energy input, and/or have negative impacts on both the environment and surfaces.[4,6] In the last two decades, great efforts have been made to develop passive anti-icing surfaces that can repel water droplets, inhibit ice formation, and reduce ice adhesion strength without external energy inputs.[7–13]

By adopting different strategies, many types of passive anti-icing surfaces have been designed and fabricated.[4] Inspired by the lotus leaf, numerous superhydrophobic surfaces (SHSs) have been developed to achieve self-cleaning properties and liquid repellency.[14,15] By engineering the hierarchical micro/nano structures, SHSs can repel incoming water droplets before freezing at a very low temperature.[16–18] The hierarchical structure can trap air between water droplets and the surface to form air pockets, which reduce the heat transfer and therefore retard ice nucleation and growth.[19] Moreover, the trapped air pockets diminish the real contact area between a surface and the eventually formed ice, and serve as crack initiators to promote detachment of ice.[20,21] As a result, the SHSs with trapped air pockets exhibit low ice adhesion strength.[22–26] Nevertheless, air pockets are not always formed on SHSs, especially in high humid environments where vapour can condense and freeze inside the surface textures thus leading to mechanical interlocking and an increase in the real contact area.[22,27–29] Even worse, the surface structure can be destroyed during removal of ice or abrasion, thereby rendering loss of icephobicity.[29] To address these challenges, *Nepenthes* pitcher plants inspired liquid infused surfaces (LISs) have been designed and fabricated.[30] The presence of defect-free, slippery liquids at the interface endows the LISs with capability to repel various liquids, maintain low contact angle hysteresis even at high pressure, and lower ice adhesion strength.[30] Unfortunately, due to the high fluidity, the lubricant at the interface can be easily removed by ice and water, resulting in dysfunction of the surface. Although many recent efforts have been made to improve the durability of LISs, they still cannot meet the requirement for practical applications.[31–33] Alternatively, soft coatings have raised interest because of their potential to reach extremely low ice adhesion strength.[34–41] Their softness induces a deformation mismatch with ice, which favours the formation of cracks at the interface and thus facilitates the separation of ice from the coating.[36,40] Although the low modulus of these coatings can enable extremely low ice adhesion, it may lead to weak mechanical durability and unwanted large deformation that can result in a dramatic increase of drag force in specific applications, *e.g.*, for wind turbines, aircraft, and ship hulls.[4] The drawbacks of these reported anti-icing surfaces call for new and better icephobic materials.

Gels are solid materials consisting of at least one substantially cross-linked network and one liquid. Depending on different liquid parts, the gels can be classified into hydrogels, organogels, ionogels, and hybrid gels, in which water, organic solvent, ionic liquid, and hybrid solvent are the dispersion media, respectively. The versatility of gels allows them to be applicable in many emerging and diverse application fields. For example, hydrogels that contain a large amount of water and tunable networks have been utilized in contact lenses, tissue

Jianying He

Jianying He received her PhD in Structural Engineering from the Norwegian University of Science and Technology (NTNU) in 2009. She has been an assistant professor at University of Science and Technology Beijing (2003–2006), a postdoctoral fellow at NTNU (2009–2011), an associate professor at NTNU (2011–2017), and since 2017, a professor in Nanomechanics at NTNU. Her current research area includes nanostructured materials, nanotechnology for petroleum engineering, and nano-enabled icephobicity.

Zhiliang Zhang

Zhiliang Zhang received his BSc and MSc from Tongji University, China, and his PhD from Lappeenranta University of Technology, Finland in 1994. He then worked as a research scientist and senior research scientist at SINTEF Materials and Chemistry, Trondheim, Norway before he was appointed as a full professor at the Norwegian University of Sciences and Technology (NTNU) in 2003. He was the founder of the NTNU Nanomechanical Lab. His research group currently focuses on material property–structure relationships, anti-icing materials, anti-gas hydrate surfaces, and nano-structured functional materials for energy applications.

engineering, sensors, electrolytes, bio-adhesives, coatings for medical devices, *etc.*[42,43] On the other hand, ionogels possess high electrical conductivity that enables the utilization as electronic skins,[44] electrolytes,[45] supercapacitors[46] and strain sensors.[47] Thanks to their unique properties in lowering ice adhesion, suppressing ice nucleation, tuning ice growth and restricting ice propagation, gels have also emerged as one of the most promising materials for anti-icing purposes very recently.[2,48–54] Given the extraordinary anti-icing potential, gels deserve dedicated efforts for further research and optimization for their wide acceptance in the anti-icing field. A review is thus in urgent need in order to consolidate the new trends and foster the development towards targeted applications.

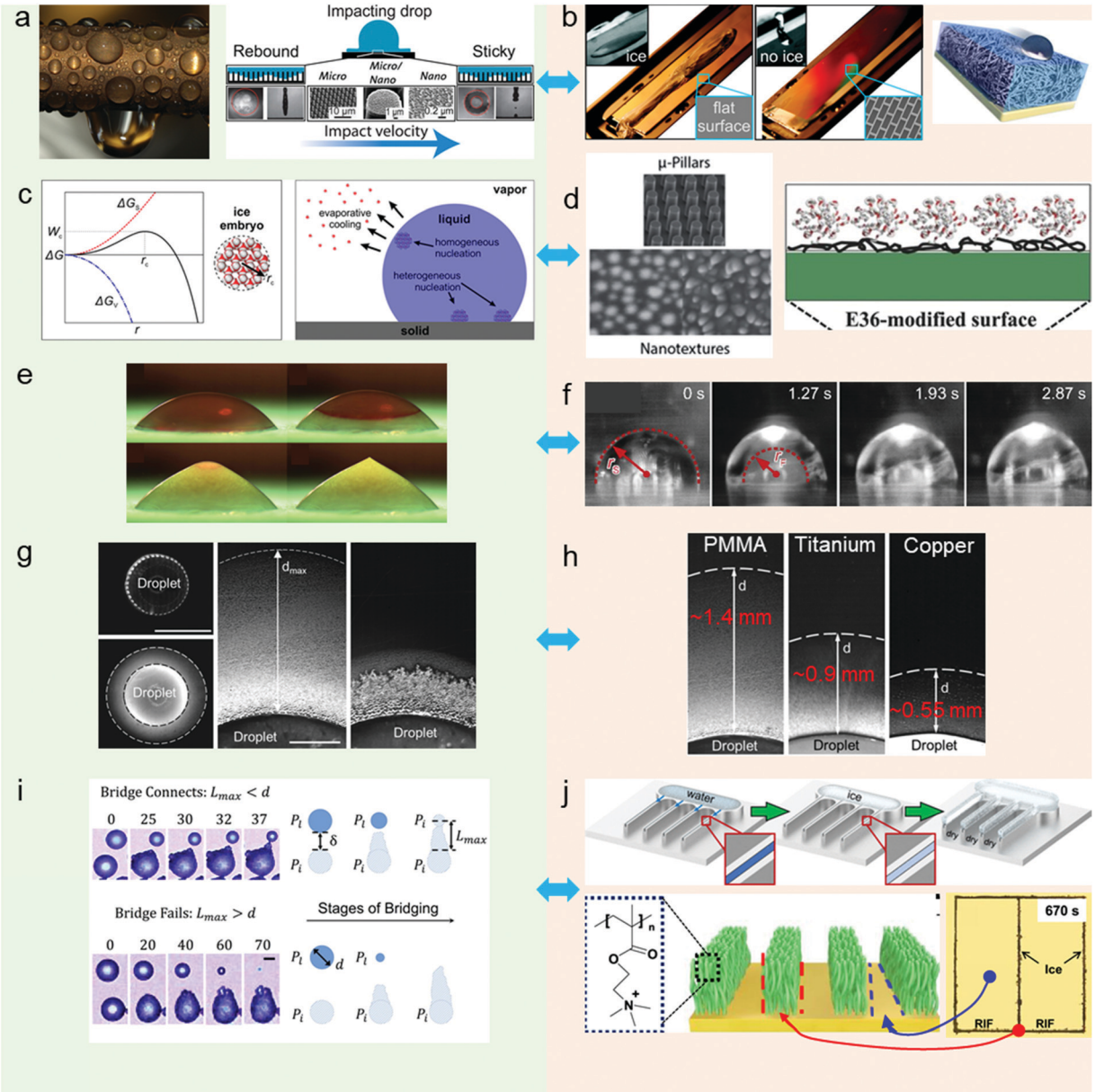

Fig. 1 From the icing process (left, light green background) to anti-icing strategies (right, light orange background). (a) Collection of water *via* condensation[56] (left; copyright 2013 American Chemical Society) and adhesion of impacting droplets[16] (right; copyright 2014 American Chemical Society). (b) Repelling water droplets by using nanostructured SHS[6] (left, copyright 2010, American Chemical Society) and LIS[30] (right, copyright 2011 Springer Nature). (c) Ice nucleation.[59] Copyright 2015 American Chemical Society. (d) Inhibiting ice nucleation by designing nanostructured surfaces (left, copyright 2014 Royal Society of Chemistry) and supercharged polypeptide surfaces (right, copyright 2016 Wiley-VCH). (e) Ice growth and recrystallization.[61] Copyright 2012 American Institute of Physics. (f) Inwards growth of ice induces spontaneous self-dislodging of droplets.[62] Copyright 2017 National Academy of Sciences. (g) Frost halos.[63] Copyright 2012 National Academy of Sciences. (h) Maximum expanse of PMMA, titanium, and copper under 1.3% humidity.[63] Copyright 2012 National Academy of Sciences. (i) Interdroplet ice bridging and dry zones.[64] Copyright 2016 American Chemical Society. (j) Restricting ice propagation by using microscopic ice patterns[65] (top, copyright 2018 American Chemical Society) and grafting patterned polyelectrolyte[66] (bottom, copyright 2020 American Chemical Society).

Herein, we first present an overview of the icing process, and briefly introduce the state-of-the-art anti-icing strategies. We then outline the latest results of anti-icing gels by categorizing them into organogels, hydrogels and ionogels, with their corresponding icephobic mechanisms, and advantages. Finally, we analyse the shortcomings of current anti-icing gels and propose suggestions for future development. We anticipate that this review can acquaint and motivate the researchers in both the anti-icing and gel research communities for rapidly advancing the understanding and fabrication of anti-icing gels.

From the icing process to anti-icing strategies

In nature, frozen water presents in various forms, including ice, snow, frost, rime, glaze, *etc.* Ice can be highly threatening to many aspects of human activities. The formation, adhesion, and accumulation of ice on exposed surfaces usually go through nucleation, growth, and then propagation stages. To avoid or ameliorate the hazard from ice accretion, different classes of passive anti-icing surfaces have been developed. An anti-icing strategy involves combating icing processes by breaking the sequential chain of events of ice accumulation.[55] In order to provide an overview of the current design principles of gels for anti-icing purposes, the state-of-the-art anti-icing strategies are summarized based on the stages of icing in this section, as shown in Fig. 1 and 2. Specifically, collection of water, ice nucleation, ice growth and recrystallization, and ice propagation *via* frost halos and inter-droplet ice bridging are highlighted on the left panels of Fig. 1 (light green background), while the corresponding anti-icing strategies are shown on the right panel (light orange background).

Avoiding adhering of liquid water

The most commonly observed unwanted icing on exposed surfaces starts from pre-existing water that is collected *via* condensation[56] (Fig. 1a, left) or adhesion of impacting water droplets (Fig. 1a, right).[16]

Removing the water before ice nucleation is a direct way to avoid unwanted ice accumulation. To repel liquid water, various types of surfaces have been developed. SHSs comprise hierarchical micro/nano structures and a low surface energy layer, showing ultra-high water contact angle (WCA $\geq$ 150 °C) and low contact angle hysteresis (CAH $\leq$ 5 °C). Therefore, they can repel incoming water droplets, thus preventing icing on their exposed face (Fig. 1b, left).[6] Since dynamic wetting behavior of water droplets on SHSs directly relates to anti-icing performance, Mishechenko *et al.* investigated the behavior of dynamic droplets impacting SHSs, and revealed that hydrophobic polymeric coatings with a closed-cell surface microstructure exhibit enhanced mechanical and pressure stability.[6] Wang *et al.* showed that the stability and water/ice repellency of SHSs can also be improved by integrating zinc oxide nanohairs onto flexible poly(dimethylsiloxane) (PDMS) micropapillae.[13] The nanohairs improve the water repellency, while the flexible PDMS cushions the impacting droplets.

Another example is LIS, which shows low CAH due to the high fluidity of the water-immiscible slippery liquid (Fig. 1b, right).[30] By proper design, even lower water sliding angles than those observed on SHS were reported.[57] The slippery liquid at the interface can not only avoid the adhering of liquid water but also lower the ice adhesion strength when ice forms on the surface.

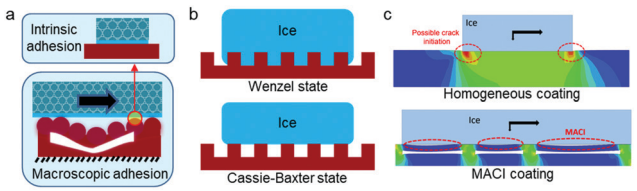

Fig. 2 Ice adhesion mechanics. (a) Intrinsic ice adhesion and macroscopic ice adhesion.[4] Copyright 2021 Elsevier. (b) Wenzel state and Cassie–Baxter state ice. Wenzel state ice forms mechanical interlocking with the surface. (c) Cracks induced by interfacial inhomogeneity. MACI: Macrocrack initiators.[36] Copyright 2017 Royal Society of Chemistry.

Inhibiting ice nucleation

Nucleation is a probabilistic event and the first step of icing, which is also the rate-limiting step for ice formation.[55] Ice nucleation generates new liquid–solid interfaces, which requires a certain degree of subcooling to overcome the free energy barrier.[58,59] As shown in Fig. 1c, the formation of an ice nucleus can be either through homogeneous nucleation or by heterogeneous nucleation, where homogeneous nucleation takes place within the liquid phase away from foreign surfaces, while heterogeneous nucleation is initiated at the liquid–solid interface.[59] The relationship between heterogeneous and homogeneous nucleation can be expressed as,[58]

$$\Delta G_{\mathrm{het}} = f(\theta_{\mathrm{iw}},R)\Delta G_{\mathrm{hom}} \quad (1)$$

where ΔG_{het} and ΔG_{hom} are the Gibbs free energy barrier for heterogeneous nucleation and homogeneous nucleation, respectively. Specifically. $f(\theta_{\mathrm{iw}},R)$ is a geometric factor and ranges from 0 to 1, meaning that the free energy barrier for heterogeneous nucleation is usually lower than that for homogeneous nucleation in the same system. θ_{iw} and R are the contact angle of ice–water and the roughness curvature radius, respectively. In addition, the ΔG_{hom} can be described by,[55,60]

$$\Delta G_{\mathrm{hom}} = \frac{16\pi\gamma_{\mathrm{iw}}^{2}}{3\Delta G_{\mathrm{f,v}}^{2}} \quad (2)$$

where γ_{iw} and $\Delta G_{\mathrm{f,v}}$ are the ice–water interfacial tension and the volumetric Gibbs free energy difference between the bulk ice and bulk water, respectively.

The physics of heterogeneous nucleation can be described by classical nucleation theory that expresses the rate of nucleation as:[60]

$$J(T) = K(T)A\exp\left(\frac{-\Delta G(T)}{k_{\mathrm{B}}T}\right) \quad (3)$$

where $K(T)$ is a kinetic prefactor representing the diffusive flux from free water molecules across the icing front interface; A, $\Delta G(T)$, k_B, and T denote the droplet–substrate contact area, the Gibbs free energy barrier, the Boltzmann constant, and the substrate temperature, respectively.

Since the free energy barrier for heterogeneous nucleation is usually lower than that for homogeneous nucleation in a given system, ice nucleation usually starts from foreign surfaces (heterogeneous). The ability to inhibit ice nucleation is usually evaluated by the nucleation delay time, which is inversely proportional to the nucleation rate, $\tau = J(T)^{-1}$. Eqn (1)–(3) show that there are several ways to inhibit heterogeneous ice nucleation: (1) decreasing the droplet–substrate contact area; (2) increasing the energy barrier by tuning the roughness curvature radius, the ice–water interfacial tension, and the volumetric Gibbs free energy difference between the bulk ice and bulk water. For example, Bai *et al.* used graphene oxide nanosheets with controlled sizes in water droplets to probe the critical ice nucleus size and demonstrated that the graphene oxide with size smaller than the critical ice nucleus can lead to a much higher free-energy barrier for nucleation, namely inhibiting the nucleation promoting effect of the graphene oxide.[67] Eberle *et al.* also showed that ice nucleation can be inhibited by tuning surface roughness and minimizing the droplet–substrate contact area (Fig. 1d, left).[60] They fabricated micro–nano hierarchical structures with micro pillars and nanopits, which reduced the droplet–substrate contact area. In addition, the prepared surfaces showed ultrafine roughness that promoted the formation of a confined interfacial quasi liquid layer between ice nuclei, leading to a change of θ_{iw}. As a result, the prepared surface exhibited a remarkable delayed ice nucleation time of 25 hours at −21 °C. Yang *et al.* prepared supercharged polypeptide (SUP) surfaces to tune ice nucleation (Fig. 1d, right).[9] They found that negatively charged SUPs inhibited ice nucleation, while positively charged SUPs promoted nucleation. It was shown that the local electric field near charged surfaces affected the water–ice nucleus interfacial tension and the volumetric Gibbs free energy difference between those of the bulk ice and bulk liquid and thus changed the energy barrier.

Controlling ice growth

Ice nucleation generates ice crystals, which form an opaque slushy mixture with the remaining liquid, followed by ice growth. Taking the freezing process of water droplets on normal surfaces as an example, as the latent heat is released through the highly conductive droplet–substrate interface, ice grows isothermally, initiating from the interface and forming a distinct pointy tip at the end (Fig. 1e).[61] During the ice growth process, the volumetric ice growth rate can be estimated by:[48]

$$\dot{V} \propto \dot{Q} \propto \frac{\Delta T}{R} = \frac{T_m - T_e}{R} \quad (4)$$

where $\dot{Q}$, ΔT, and R are the heat flux, the temperature difference between the melting temperature (T_m, 0 °C for pure water) and the substrate/environment temperature (T_e), and the thermal resistance between the substrate/environment and the freezing front, respectively. The growth direction is inverse to the major heat release direction.

The time for completing ice growth is usually orders of magnitude shorter than the ice nucleation delay time. Thus, there are only a few studies reported on prolonging the ice growth time. According to eqn (4), the ice growth rate is related to the environmental temperature and the thermal resistance between the environment and freezing front. This means that the ice growth time can be increased by enhancing the thermal resistance of the heat release channel. For example, Shen *et al.* demonstrated that the micro–nanoscale hierarchically structured superhydrophobic surface not only inhibited ice nucleation due to the decreased actual solid–liquid contact area, but also lowered the ice growth rate owing to the insulating action caused by the trapped air pockets.[19]

Notably, because the ice growth direction is opposite to the major heat release direction, the growth direction can also be altered by changing the temperature difference. By controlling the substrate temperature and increasing the heat convection, ice can grow from the droplet–air interface to droplet–substrate interface, leading to the so-called self-dislodging of formed ice (Fig. 1f).[62] However, such a phenomenon requires artificial control of the substrate temperature and environmental conditions, which is not appliable in realistic situations.[48]

In addition, the wettability of solid surfaces also influences the pattern of ice growth in the condensation-frosting process.[68] Liu *et al.* reported the successful controlling of ice growth by altering the wettability of the solid surface.[68] On a hydrophilic surface, ice favoured an along-surface growth mode due to the presence of bilayer hexagonal ice with an optimized matching basal face and thus promoted rapid ice growth rate, whereas ice on a hydrophobic surface showed an off-surface growth mode, which resulted in weak adhesion between the formed ice crystals and the solid surface.

Restricting ice propagation

The coverage of ice on a surface is usually realized through the inter-droplet interactions rather than individual freezing of droplets. This process is the so-called ice propagation. The freezing of a droplet can initiate ice propagation *via* either frost halos or inter-droplet ice bridging. To avoid ice covering a whole surface when the water droplet freezing is inevitable, ice propagation should be restricted.

Frost halos is a phenomenon that occurs during freezing of a droplet. The latent heat during ice nucleation is released to the remaining liquid, and thus induces its evaporation. Due to the lower temperature of the substrate, vapor can subsequently condense or even freeze on the substrate close to the frozen droplet (Fig. 1g).[63] These frost halos may render the freezing of nearby droplets through a domino effect. Alternatively, the explosive latent heat will also be released through the substrate, which mitigates the evaporation of the remaining liquid. As such, increasing the thermal conductivity of the substrate can suppress the frost halos and minimize the ice propagation.[63,69] Jung *et al.* have revealed that higher thermally conductive surfaces can form a smaller frost halo due to the faster removal

of latent heat, and thus have lower possibility of freezing of neighbouring droplets (Fig. 1h).[63]

Inter-droplet ice bridging is another phenomenon that could lead to ice propagation.[55] The saturated vapor pressure over frozen droplets is lower than that over liquid droplets at the same subfreezing temperature, resulting in localized vapor pressure gradients in the system where the frozen droplets serve as local humidity sinks.[55] In addition, the heat released by freezing will conduct to the neighbouring droplets *via* the substrate, leading to localized temperature gradients.[66] Both localized vapor pressure gradients and temperature gradients cause the mass transfer from liquid droplets to the frozen one, namely the water molecules evaporate from the liquid droplets and then deposit on the frozen droplets. As shown in Fig. 1i, during this process, the frozen droplet grows towards the adjacent liquid droplets that are being harvested, forming ice crystals.[55,64] The liquid droplets will start freezing once the formed ice crystals contact them, forming ice bridges to connect droplets to form a network. However, the ice bridge will fail when the distance between the edge of the frozen droplet and the centre of the liquid droplet (L_{max}) is larger than the original diameter of the liquid droplet (d), leading to a dry zone.[64]

The way to break ice bridging is to control the distance between the frozen and unfrozen droplets. As discussed previously, the ice bridge will fail when the distance between the edge of the frozen droplet and the centre of the liquid droplet (L_{max}) is larger than the original diameter of the liquid droplet (d). The frozen droplets will harvest the neighbouring water droplets and thus create an annular dry zone around the formed ice. Spatially controlling ice formation through surface patterning, wettability tuning, and polymer grafting can cause the inter-droplet bridging to fail and create large ice-free areas (over 90% of the exposed surface).[65,66,70,71] For example, Ahmadi *et al.* have designed aluminium surfaces with microgrooves for reserving water, which can freeze to ''ice stripes'' under chilled conditions (Fig. 1j, top).[65] The ''ice stripes'' harvest water vapor in the nearby regions and then leave the surface with more than 90% of ice-free area. On surfaces with macrotexture[70] and microgroove patterns,[71] an increasing gradient of water vapor concentration from the bottom to the top of the surface topography can be formed thanks to the local structural confinement effect. Thus, vapor condensation and frost formation are preferred on the upper tip of the surface structure. The formed frost constantly collects vapor from the condensed droplets in the local valley due to the vapor pressure difference, and consequently breaks the inter-droplet bridging and stops ice propagation. Ice propagation can also be guided by tailored surface local properties. Jin *et al.* prepared patterned polyelectrolyte coatings to inhibit condensation freezing (Fig. 1j, bottom).[66] The prepared poly[2-(methacryloyloxy)-ethyltrimethylammonium iodine] brushes on the surface promoted ice nucleation, leading to the earlier formation of ice on the grafted area. Due to the low vapour pressure over ice, water vapour favoured depositing on the formed ice. In addition, during the freezing process, the latent heat was released to the substrate, facilitating the evaporation of the neighbouring water droplets. For the best result, an ice-free zone of up to 96% of the whole surface area can be achieved.

Reducing ice adhesion

After formation of ice, the most effective strategy to ameliorate the hazard from ice accretion is to reduce ice adhesion, and in an ideal case letting the formed ice be automatically removed by natural forces, *e.g.*, gravity and wind. With different scales, ice adhesion can be described by intrinsic and macroscopic adhesion, as shown in Fig. 2a.[4] Intrinsic adhesion is a result of the atomistic attraction of water/ice molecules to a surface in the form of Coulombic and van der Waals forces.[72–75] The origin of intrinsic adhesion implies that the following methods can be used to reduce ice adhesion: (1) to weaken the atomistic interactions between the surface and water molecules by lowering the surface energy and increasing the hydrophobicity of the surface; (2) to destabilize the contact between surface and water molecules by introducing an insulating layer. Meuler *et al.* have shown that ice adhesion strongly correlates with water wettability ($\tau \propto 1 + \cos\theta_{rec}$, where τ and θ_{rec} are ice adhesion strength and the water receding contact angle, respectively).[76] Although the correlation fails for surfaces with ice adhesion strength larger than 60 kPa, it demonstrates the possibility of tuning ice adhesion by method (1).[77] To lower the surface energy, fluorine-containing polysiloxanes are usually chosen as the coating materials.[4,78] LIS as an example for method (2) can lower ice adhesion since the slippery liquid layer serves as a barrier to avoid the direct contact of ice and substrate.[30] LIS can be fabricated by infusing different lubricants (silicone oil,[79] perfluoroalkylether,[80] and liquid paraffin[31]) into porous structures or polymeric networks. The abundant lubricant forms a stable, defect-free, and slippery layer, which serves as an insulating layer between ice and the substrate. The slippery nature of the infused lubricant grants the prepared surface with low adhesion to ice.

Given that real surfaces are usually rough on different length scales, there are always voids at the ice–surface interface. These voids can function as crack initiators, create stress concentration, and thus affect the interface crack propagation. Macroscopic adhesion is thus a function of the intrinsic adhesion and interface cracks. According to fracture mechanics, the critical strength to separate two solid surfaces can be approximated as: $\tau = \sqrt{EG/(\pi a \Lambda)}$, where E, G, a, and Λ are the elastic modulus, surface energy, crack length and a non-dimensional constant related to geometric configuration, respectively.[36,38,81] The equation indicates that tuning the features of voids by altering surface roughness and controlling deformation incompatibility (such as modulus mismatch between ice and surface[40] as well as modulus mismatch in different regions of surface[36,82]) can also reduce the ice adhesion strength. For example, due to the presence of micro/nano surface structures, some SHSs can not only reduce the contact areas/points controlled by intrinsic adhesion but also facilitate the initiation and propagation of interface cracks.[20,21] The prerequisite for these SHSs with

reduced ice adhesion is the existence of a Cassie wetting state, which is affected by the size and topography of the micro-voids (Fig. 2b). Alternatively, designing and controlling the properties and morphologies of sub-surface structures can promote the formation of interface cracks and significantly lower the ice adhesion strength.[34,36,37] As shown in Fig. 2c, He *et al.* prepared a soft PDMS coating with macroscale substructures under the surface.[36] The presence of the macroscale substructures facilitated the formation of voids at the interface because of deformation incompatibility, resulting in a super-low ice adhesion strength (5.7 kPa). Coincidentally, Irajizad *et al.* introduced ultrasoft gel fillers into a PDMS matrix to achieve modulus mismatches in different surface regions, which render stress localization and deformation incompatibility during de-icing.[82]

Anti-icing gels

Based on the above analyses of icing processes and anti-icing strategies, it can be easily seen that gels have great potential to be used as anti-icing materials. First, the large amount of liquid existing in the gels offers the possibility to form an interfacial liquid layer that naturally weakens the intrinsic ice adhesion.[83,84] Second, its low surface elastic modulus can induce a distinct stiffness mismatch between the ice and substrate, which promotes the initiation of interface cracks and thus drastically lowers the ice adhesion strength.[40,41] Moreover, the versatility of the available liquids and cross-linked networks provides many alternatives for controlling ice nucleation, ice growth and even ice propagation. The physical properties of gels are usually dominated by the species of their liquid part, *e.g.*, hydrogels are often hydrophilic because of the abundant water; ionogels display high electrical conductivity due to the presence of conductive ionic liquid. Therefore, in the following, we summarize the performances and mechanisms of current anti-icing gels by their liquid base, *i.e.*, organogels, hydrogels, and ionogels.

Organogels

The large amount of organic liquids inside organogels leads to extremely low density of elastic strands and elastic modulus values 2–3 orders of magnitude lower than that of ice.[4,85] The giant modulus mismatch between organogels and ice grants those gels ultralow ice adhesion due to the deformation incompatibility during de-icing (Fig. 3a).[40] As shown in Fig. 3b, Beemer *et al.* prepared gels consisting of cross-linked PDMS networks and different amounts and molecular weights of non-reactive trimethyl-terminated PDMS (*t*-PDMS).[40] The results showed that ice adhesion follows $\tau = \sqrt{W_{adh}\mu/t}$, where W_{adh}, μ, and t are the work of adhesion between ice and the coating, shear modulus and thickness of the coating, respectively. They also demonstrated the formation and propagation of air cavities at the ice-coating interface. Although the PDMS gels exhibit ultralow ice adhesion strength, the low modulus may lead to weak mechanical durability and an unwanted large deformation during specific applications, *e.g.*, for wind turbines, aircraft, and ship hulls.[4]

The other functionality of organogels for anti-icing is their lubricant-secretion ability. The crosslinking reaction of PDMS in the presence of other organic liquids can lead to an increase of the free energy of mixing (ΔG_{mix}), resulting in demixing of the organic liquid and the PDMS matrix (if $\Delta G_{mix} > 0$).[84] As shown in Fig. 3c, the syneresis effect continuously generates a liquid layer on the top of the prepared organogel surfaces under certain conditions. The formed liquid layer can serve as an insulating layer to mitigate the intrinsic adhesion, consequently achieving extremely low ice adhesion (*ca.* 0.4 kPa).[84] Such a low ice adhesion enables the autonomous sliding of ice pillars off a slightly inclined surface. The organogels reported above are prepared by an *in situ* method, in which cross-linking and infusing occur at the same time. A post-infused method, infusing lubricant after cross-linking, can also be applied to prepare organogels with ultra-low ice adhesion strength. Wang *et al.* demonstrated that liquid paraffin can be infused into cross-linked PDMS networks at an elevated temperature.[83] After cooling down to room temperature, the surface of the prepared organogel is covered by a thin layer of paraffin that is released from the bulk PDMS networks due to the osmotic pressure driven by the temperature change. The continuous release of paraffin makes the organogel display ultra-low ice adhesion even after 35 icing/deicing cycles and 100 days of environmental exposure. By incorporating such thermoresponsive property into organogels, other surfaces with switchable interfacial properties are designed and fabricated for anti-icing applications.[52,87] Urate *et al.* used micro/nanostructured moulds to prepare textured organogel films consisting of cross-linked PDMS as the matrix and polymethylphenylsiloxane (PMPS) as the lubricant.[87] By tuning the ratio of PMPS and PDMS, the critical syneretic temperature (CST) can be varied from −15 to 50 °C. When the temperature is lower than CST, PMPS is spontaneously secreted to the topmost layer of the gel, forming a slippery surface, which contributes to excellent icephobic performance. In the meantime, PMPS on the surface gradually is absorbed into the polymer networks when the temperature is above the CST. The release of oil also induced a change of optical properties since the released oil can bury the surface micro/nanotextures. By infusing a binary liquid mixture with an upper critical solution temperature into a polymer network, Ru *et al.* fabricated a reversibly thermoresponsive organogel (Fig. 3d).[52] The critical phase separation temperature was tuned by varying the composition. Due to the phase separation ability during temperature change, the organogels can reversibly secrete/absorb liquid, and thus exhibit a switchable lubricating property. The organogel in the lubricating state showed extremely low ice adhesion (<1 kPa).

Although the above organogels with a lubricant surface present ultralow ice adhesion, the easy depletion of liquid lubricant may pollute the environment and lead to poor durability. To improve the durability of anti-icing organogels, liquid lubricants can be replaced by solid organic ones, which mitigate the loss of the sacrificial layer.[86,88] Following such a concept, alkane[86] and perfluoroalkane[88] have been infused into the PDMS matrix at a temperature higher than their melting

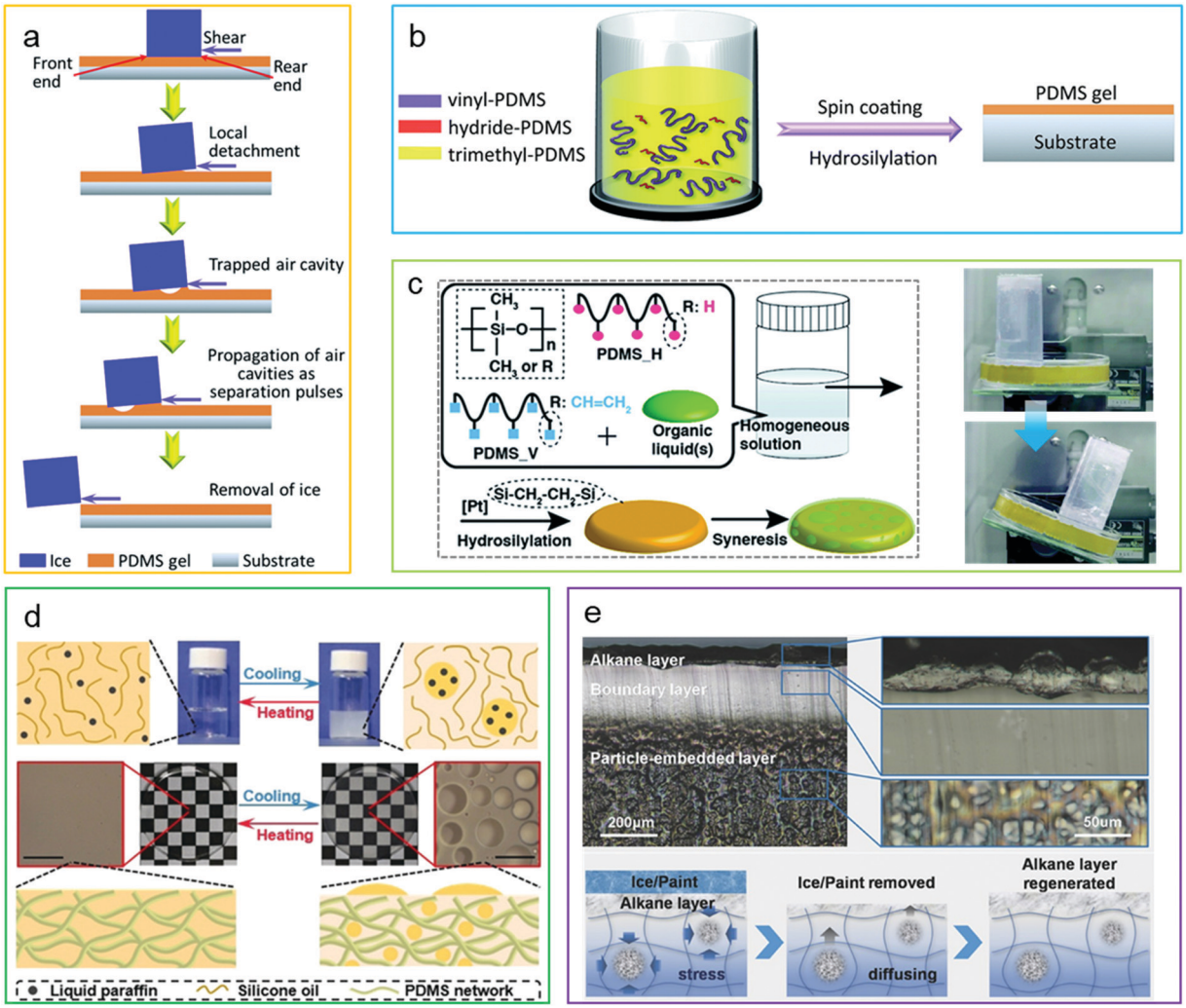

Fig. 3 Anti-icing organogels. (a) Formation of cavities at the interface between ice and soft organogels during deicing.[40] Copyright 2016 Royal Society of Chemistry. (b) Preparation of PDMS organogels.[40] Copyright 2016 Royal Society of Chemistry. (c) Crosslinking syneresis of PDMS induces secretion of organic liquids, enabling autonomous sliding off of ice on a slightly inclined surface.[84] Copyright 2015 Royal Society of Chemistry. (d) Phase separation of liquid paraffin/silicone oil solution and phase separation of reversibly thermosecreting organogels.[52] Copyright 2020 Wiley-VCH. (e) Solid organogels with a regenerable sacrificial alkane surface layer.[86] Copyright 2017 Wiley-VCH.

points. During the infusing process, a sufficient amount of solid lubricant will cause the swelling of the elastomer matrix, and then induce the gradient of both the concentration and the stress after cooling down to room temperature or even lower temperature. As a result, the solid lubricant inside the elastomer matrix can be squeezed out to the topmost surface layer when the top sacrificial layer is being damaged or removed (Fig. 3e).[86] The solid nature and regenerability synergistically improve the durability of the prepared organogels. Though the durability of solid organogels have been greatly improved, the consumption of lubricant will eventually render the loss of icephobicity.

By incorporating dynamic bonds into the polymer networks of an organogel, new functionality, *i.e.*, self-healing, can be obtained to further improve the mechanical durability.[89,90] Due to the reformation ability of the broken dynamic bonds (hydrogen bonds, disulfide bonds, metal–ligand coordination, *etc.*), the prepared organogels can repair mechanical cuts and scratches. It should be noted that the presence of liquid medium in supramolecular networks can accelerate the chain mobility, and thus promote the reconstruction and reversible exchange of dynamic bonds, leading to a high self-healing efficiency.[89]

Hydrogels

Hydrogels contain a large amount of water, which has a freezing point around 0 °C (at normal atmosphere). Therefore, common hydrogels usually show poor freezing resistance to low temperature. However, by introducing additives and modifying the polymer networks, hydrogels can maintain their softness and other gel characteristics at sub-zero temperatures.[91] The modified hydrogels are the so called anti-freezing hydrogels. It is envisaged that anti-freezing hydrogels also work for anti-icing purposes since the interfacial non-frozen water can not

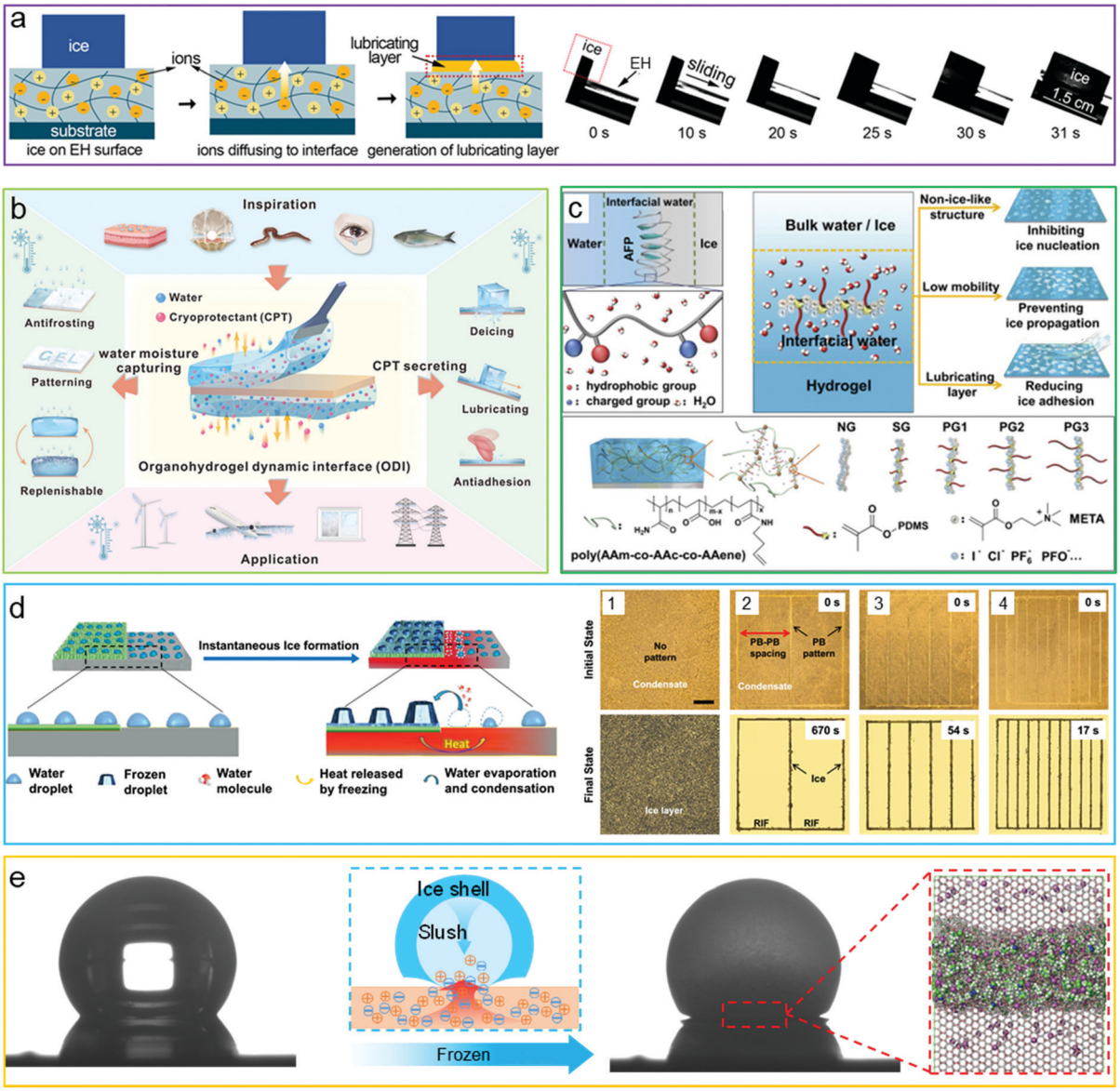

Fig. 4 Anti-icing hydrogels and ionogels. (a) Electrolyte hydrogel surfaces melt the ice at the interface to form a lubricating layer, which enables the automatic sliding off of ice.[50] Copyright 2020 American Chemical Society. (b) Hydrogels consist of CPTs inspired by mucus secretion towards applications at sub-zero temperatures.[51] Copyright 2020 American Chemical Society. (c) Bioinspired multifunctional anti-icing hydrogel.[2] Copyright 2020 Elsevier. (d) Patterned hydrogel surface prevents the propagation of ice, resulting in large ice-free zones.[66] Copyright 2020 American Chemical Society. (e) Unconventional inward ice growth on ionogel surfaces leads to a spherical cap and a concentrated ionic liquid aqueous interface.[48] Copyright 2020 American Chemical Society.

only serve as a lubricant for lowering ice adhesion but also tune ice formation, including ice nucleation and ice propagation.[2,49–51] These hydrogels can be categorized by their synthesis strategies, *i.e.*, (1) introduction of additives, and (2) modification of polymer networks.

It is known that salt solutions exhibit depressed freezing points below 0 °C. For example, an aqueous solution with 23.3% of NaCl shows a suppressed freezing point of −21.1 °C.[92] Therefore, salt is often used to melt ice and snow on pavements to prevent traffic accidents. Taking the advantage of freezing-depression by salt, Li *et al.* developed electrolyte hydrogel (EH) surfaces by introducing salts into poly(vinyl alcohol) hydrogel for anti-icing, as shown in Fig. 4a.[50] By tuning the concentration and species of salt, the EH surfaces demonstrate an ability to prevent ice/frost formation and reduce ice adhesion to Pascal-level even at a low temperature of −48.8 °C. Due to the ultralow ice adhesion, the formed ice on the EH surface can be removed by gravity. Because the salt of EH can be replenished with various ion sources, *e.g.*, seawater, the prepared EH surface shows great potential for applying on offshore infrastructures and ship hulls. In addition to salts, many organic compounds, such as ethylene glycol, propylene glycol, glycerol, and dimethyl sulfoxide have also been utilized for freezing-point depression of water for cold environments,

e.g., cryopreservation.[93,94] Inspired by mollusks, which can secrete mucus on their skin surface to adapt to environmental change and protect themselves, Chen *et al.* prepared hydrogels containing a large amount of cryoprotectants (CPTs, *e.g.*, glycerol and ethylene glycol) *via* a solvent-displacement method (Fig. 4b).[51] The CPTs inside the gel matrix dynamically exchanged with the water and then melted the ice at the interface to form a liquid layer that is highly favourable for both resisting frosting formation and facilitating low ice adhesion. Unfortunately, these anti-icing hydrogels continuously lose the crucial additives during usage, rendering their ultimate dysfunction in due time.

Based on the mobility and freezing temperatures of water, water molecules inside the hydrogels exist in one of the three states, *i.e.*, unfrozen water, weakly bound water, and free water,[91,95–97] depending on their interactions with polymer networks. Unfrozen water interacts strongly with polymer networks, thus possessing weak mobility and extremely low freezing temperature, even down to −100 °C. Weakly bound water has relatively low interaction with the polymer matrix; their mobility is therefore partly restricted by the polymer network. Consequently, they can remain in the amorphous state slightly below 0 °C. Free water is the water that has almost no interaction with the polymer networks and shows the same freezing temperature as bulk water outside the hydrogel (∼0 °C). Since the states of water in hydrogels highly depend on the interactions of water molecules with polymer segments, it is feasible to tune the water states by designing and modifying the polymer networks.[2,49,53] Inspired by anti-freezing proteins, He *et al.* prepared PDMS-grafted polyelectrolyte hydrogels for anti-icing purposes.[2] As shown in Fig. 4c, by tuning the arrangement of hydrophobic PDMS and charged functional groups, the hydrogel can mimic the function of anti-freezing proteins in maintaining a non-frozen interfacial water layer. The resulting interfacial water grants the hydrogel coating multifunctional anti-icing properties. The ice nucleation on the designed hydrogel surface is inhibited (ice nucleation temperature < −30 °C), because the optimized charge groups restrict the structural transformation of water from liquid-like to ice-like.[98] The ice propagation is also hindered by the altered ice–solution interfacial tension, which can be tuned by hydrophobic chains and ion species.[10,69] The synergetic cooperation of hydrophobicity and ion specificity leads to effective restricted ice propagation rate.[2] In addition, the interfacial water can also serve as a lubricant to reduce the ice adhesion below 20 kPa. Altering crosslinking degree is another way to control the generation of interfacial water. In a fully hydrated hydrogel, the internal fraction of unfrozen water increases with the crosslinking degree because the internal polymer networks restrict the mobility of water molecules.[99–101] Huang *et al.* showed that the freezing temperature on a cross-linked hydrogel (cross-linked dopamine-grafted sodium alginate, SA-*g*-DA) decreases with crosslinking degree.[49] Besides, crosslinking and grafting of dopamine grant the hydrogel with excellent stability and good adhesion on many types of solid surfaces, respectively.

In addition to bulk hydrogel coatings, surface-patterned hydrogels have also been designed for localized controlling of the ice formation.[66,100] Ice-nucleating proteins (INPs) found in many freeze-tolerant species promote ice nucleation in the extracellular spaces.[102,103] The formed ice harvests water from the intracellular spaces due to lower vapor pressure of ice compared with that of water, which can prevent intracellular freezing.[100] Inspired by such freeze-tolerant organisms, patterned polyelectrolyte hydrogel (PH) surfaces[66] and patterned hydrogel-encapsulated INPs (PHINPs)[100] were developed, both displaying excellent ability to inhibit ice propagation. The ice nucleation temperature of the hydrogel was increased by tuning the counterions of hydrogels or encapsulating INPs into poly(acrylamide-*co*-2-hydroxyethyl methacrylate) hydrogels. As shown in Fig. 4d, the increased nucleation temperature led to the preferential formation of ice stripes on the coated area of the sample surface. Due to the lower vapour pressure over ice, the water vapour deposited on the formed ice. In addition, the latent heat was released to the substrate during freezing, facilitating the evaporation of neighbouring condensate water droplets. As a result, large ice-free zones can be achieved (Fig. 4d).[66,100]

Although hydrogels mentioned above present excellent icephobicity, their functionality relies on the state of interfacial water, which is strongly affected by temperature. At an extremely low temperature, it is challenging to keep the interfacial water in an amorphous state.[11,104]

Ionogels

Ionogels consist of polymer networks and ionic liquids. Thanks to the huge diversity of ionic liquids, the category of gels exhibits great versatility. By selecting various polymer networks and ionic liquids, ionogels have been widely utilized as self-cleaning surfaces,[105] stretchable ionic conductors,[106] electronic skins,[44] electrolytes for batteries,[45] and flexible supercapacitors.[46] According to their interaction with water, ionic liquids can be divided into hydrophilic and hydrophobic.[105]

Although ionogels containing hydrophobic ionic liquids demonstrated excellent water repellency due to the lubrication effect,[105] their possible application in the anti-icing field is surprisingly not reported. Hydrophilic ionic liquids are known for their capacity of freezing-point depression, which guarantees the corresponding ionogels as promising candidates for anti-icing applications.[107] Zhuo *et al.* designed and prepared anti-icing ionogels consisting of crosslinked gelatin and 1-butyl-3-methylimidazolium bromide (BMImBr).[48] Due to the effective freezing-point depression of BMImBr, the ionogel surface can not only inhibit ice nucleation, but also alter the ice growth direction of the water droplets on the surface at subzero temperatures. As shown in Fig. 4e, the unconventional inward ice growth from the droplet–air interface to droplet–ionogel interface leads to spherically capped ice rather than normal pointy capped ice. Because of the inward growth and brine rejection at the freezing front, a concentrated ionic liquid aqueous layer can form at the ice–ionogel interface, enabling an ultralow ice adhesion. In addition, since the ionogel can

absorb the water molecules even in cold environments to generate a non-frozen liquid layer on the surface, the prepared ionogel also exhibits remarkable anti-frost properties. However, the possible exhaustion of ionic liquid during application can result in the loss of icephobicity.

It is worth noting that the anti-icing applications of ionogels are currently limited, because their anti-icing potentials have started to be appreciated very recently and the leakage of some ionic liquids is hazardous to the environment.[48] Nevertheless, such environmental issues could be overcome by using green ionic liquids. Given the great variety of both ionic liquids and polymers available, there is an almost unlimited number of combinations of the two for fabricating new anti-icing ionogels. In addition, the unique features of ionic liquids can bestow new functions on ionogels. For example, the high electrical conductivity of ionogels can be an ideal property for enabling electrothermal anti-icing and other electroresponsive potentials. As encouraging results further broadcast,[48] ionogels can be as popular as, if not more favourable than, the other two gel types for anti-icing.

Summary & perspective

In this review, we firstly iterated the key events in icing and current anti-icing strategies to break the sequential chain of icing processes. We then surveyed the state-of-the-art gels that were designed and fabricated for anti-icing purposes. The current anti-icing gels were categorized into organogels, hydrogels, and ionogels for the convenience of referencing in future relevant studies. The comparison between these anti-icing gels is further outlined in Table 1. Overall, all the current anti-icing gels suffer from the common drawbacks of poor liquid retention ability, weak adhesion to substrates, and low strength as well as low toughness. Most of the organogels achieve anti-icing properties by incorporating interfacial lubricant layers to weaken the intrinsic adhesion. However, the liquid lubricant layers can be easily depleted, leading to poor durability. To improve the durability of anti-icing organogels, solid organogels, self-healing organogels, and thermoresponsive organogels can be developed. The interfacial water in hydrogels plays a crucial role in the anti-icing performance.

Non-frozen water of hydrogels can be achieved by introducing additives or modifying polymer networks, resulting in a slippery surface for lowering ice adhesion. In addition, ice nucleation can be controlled by tuning the charge groups in hydrogels. Bulk hydrogels that can inhibit ice nucleation and patterned hydrogels that can promote ice nucleation have been designed for anti-icing applications. However, the state of water is strongly influenced by the temperature. At an extremely low temperature, it becomes highly challenging to keep the interfacial water in the amorphous state.[11] The patterned hydrogels show preferential formation of ice, and thus can harvest the water molecules from the atmosphere and the other surface areas without hydrogels, and consequently lead to large ice-free zones. Anti-icing ionogels can not only inhibit ice nucleation but also alter the ice growth direction on their surfaces, which is enabled by the presence of ionic liquid and the resulting depressed freezing-point. In summary, though the current anti-icing gels still suffer from some major demerits, *e.g.*, poor durability, their remarkable anti-icing performances signify a promising future (Fig. 5a). In order to promote the development of gel-based anti-icing surfaces, we have identified the following paths for further research, including pathways to enhance durability, the need to build up the missing fundamentals, and the possibility to enable stimuli-responsive properties.

Durability

Weak durability of anti-icing gels results from the poor mechanical robustness, adhesive failure to the substrate, and/or depletion of liquid phase or additives. The poor mechanical robustness of the current anti-icing gels is rooted in the low areal density of polymer strands and the lack of a toughening strategy.[85] Fortunately, many approaches have been developed to toughen polymer networks, such as incorporating energy dissipation networks, designing double networks, and adding fillers (Fig. 5b),[108] which can also be adopted to design tough and strong anti-icing gels.[2,48] Another obvious challenge for the anti-icing gel coatings is the weak adhesion to substrates due to

Table 1 Comparison of different types of anti-icing gels

Materials	Major contents	Mechanisms	Drawbacks	
			Individual	Common
Organogels	Organic compound	Deformation incompatibility	Limited application scenarios, *e.g.*, deformation of coating can dramatically increase the unwanted drag force of wind turbines, aircraft, and ship hulls	Poor liquid retention ability; weak adhesion to substrates; low strength; low toughness
		Lubrication	Easy to be evaporated and drained away; environmentally unfriendly	
Hydrogels	Water	Freezing point depression additives	Additives are easy to be removed away; environmentally unfriendly	
		Interfacial water control by network design	Strong temperature dependence	
Ionogels	Ionic liquid	Freezing point depression	Ionic liquids are easy to be removed by water; environmentally unfriendly	

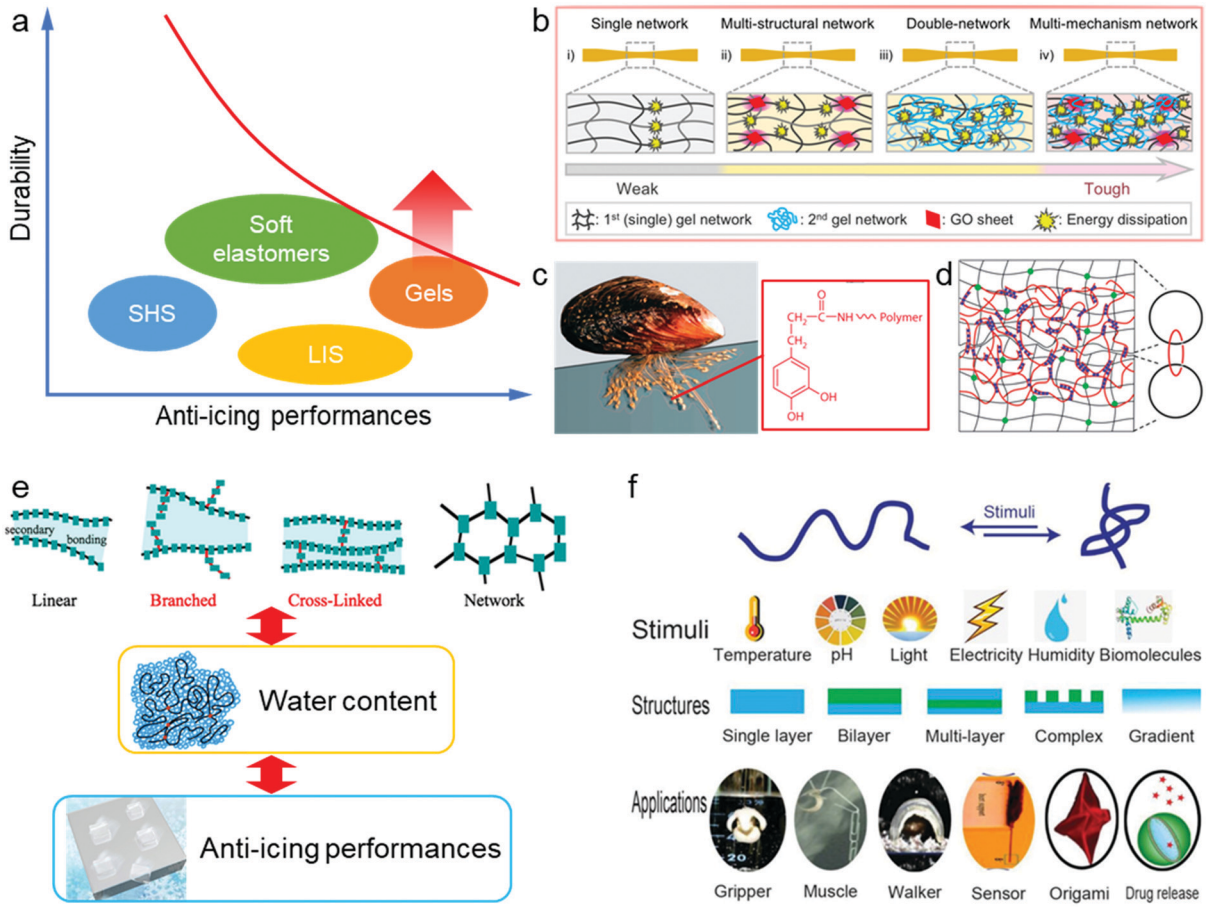

Fig. 5 Perspectives of anti-icing gels. (a) Anti-icing performances and durability of current anti-icing materials denote the improving direction of anti-icing gels. (b) Toughening strategies of gels by introducing a second network, nanofillers and energy dissipation mechanisms.[108] Copyright 2020 Springer Nature. (c) Enhancing the adhesion of gels to substrates by mimicking essential features of the adhesive chemistry practiced by mussels.[109] Copyright 2001 Annual Reviews. (d) Designing topological networks to increase the adhesion between gels and dry polymers.[110] Copyright 2018 Wiley-VCH. (e) The relationships between polymer networks, water content and anti-icing performances are awaiting to be discovered.[11,111,112] Copyright 2020 Elsevier and 2014 Wiley-VCH. (f) The changeable properties of stimuli-responsive materials support various applications.[113] Incorporating external stimuli-responsive properties into anti-icing gels will widen the applications and hold great promise to address current defects. Copyright 2019 Wiley-VCH.

the wet surfaces that result from the liquid phase of gels.[114,115] The weak adhesion may be addressed by mimicking essential features of the adhesive chemistry practiced by mussels (Fig. 5c)[109] and/or designing topological adhesion (Fig. 5d).[110,116]

In addition to the weak mechanical durability, the drain of liquid phases or additives is also a reason for the dysfunction of anti-icing gels. Due to the high fluidity, the liquid in gels may leak out, thus leading to the loss of anti-icing performance. The evaporation of the liquid part (especially water) will render the loss of functionality as well. Some gels diffuse functional molecules to the interface to achieve outstanding anti-icing performance; however, it comes at the cost of the diffused molecules being removed by water at the same time. Such a process may not only be detrimental to the long-term stability but also contaminative to the environment.[48,91] Although replenishing salt from seawater has been adopted to improve the sustainability, the application conditions of the corresponding gel were still limited to marine areas.[50] Therefore, new advanced techniques should be developed for retaining the liquid phase and additives. Developing polymer networks with high affinity to additives and immobilizing anti-freezing groups may mitigate the loss of functional components.

Fundamentals of anti-icing gels

In order to address the weak durability and maintain the outstanding anti-icing performances at the same time, it is vital to unravel and understand the fundamentals of anti-icing gels. In a previous work, the complex relationship between crosslinking density, water content and anti-icing properties of gels has been investigated,[49] which provides clear guiding directions for the future optimization and exploration of new anti-icing gels. Polymer brushes with various hydrophilic backbones and different length of hydrophobic side chains have been developed to mimic anti-freezing proteins, and the relationship between the molecular groups, water states and anti-icing performances has been studied.[2] Given that the anti-icing gel is still in its infancy, the most urgent need would be to enlarge the sample populations and to enrich the

corresponding anti-icing result database. Taking the anti-icing ionogels for example, accumulating a sufficiently large number of validated results can enable other powerful methodologies, such as machine learning, to participate in the relevant selection of ionic liquids. By doing so, concealed fundamentals of gels that are crucial to anti-icing can be revealed. Entangling puzzles, for example how the different polymer networks (linear including random and block, branched, cross-linked, *etc.*) affect the water content (unfrozen water, weakly bound water, and free water) and thus anti-icing ability (Fig. 5e),[11,111,112] and how the functional groups (their species and grafting density) influence the water states and anti-icing properties, can be solved.

External stimuli-responsive properties

External stimuli-responsive materials have attracted substantial attention thanks to their changeable properties towards various applications, *e.g.*, responsive coatings, controllable liquid-repellency, and adaptive shape memory materials.[113,117,118] Such external stimuli-responsive properties can also endow the anti-icing gels with dynamic nature, unstable interface, and thus reversible interaction with ice. In addition, on-demand response allows the loss of the functional agent during usage to be reduced and therefore enhances the durability. Hence, it is important to develop smart anti-icing gels. Unfortunately, only a few relevant studies on external stimuli-responsive anti-icing gels have been reported to date. For example, thermoresponsive properties have been introduced into organogels to enhance the on-demand secretion of lubricants to the surface and to improve the anti-icing abilities and durability.[52,87] It should be noted that not only the temperature but also many other ambient conditions can serve as external stimuli. By designing polymer networks and incorporating nanoparticles, stress, light, electrical field, and magnetic field can also trigger changes in the gel properties (Fig. 5f).[113,118] We envision that such smart anti-icing gels with predictable and changeable properties will widen the applications and hold great promise to address the current defects.

Conflicts of interest

There are no conflicts to declare.

Acknowledgements

The Research Council of Norway is acknowledged for the support to the PETROMAKS2 Project Durable Arctic Icephobic Materials (No. 255507) and the Dandra Project (No. 302348). J. C. acknowledges the support by the National Natural Science Foundation of China (No. 21676133). T. L. thanks the support by the National Natural Science Foundation of China (No. 12002350), and the CAS Key Laboratory of Bio-inspired Materials and Interfacial Science, Technical Institute of Physics and Chemistry, Chinese Academy of Sciences.

References

1 K. Golovin, A. Dhyani, M. D. Thouless and A. Tuteja, *Science*, 2019, **364**, 371–375.
2 Z. Y. He, C. Y. Wu, M. T. Hua, S. W. Wu, D. Wu, X. Y. Zhu, J. J. Wang and X. M. He, *Matter*, 2020, **2**, 723–734.
3 Y. Shen, X. Wu, J. Tao, C. Zhu, Y. Lai and Z. Chen, *Prog. Mater. Sci.*, 2019, **103**, 509–557.
4 Y. Zhuo, S. Xiao, A. Amirfazli, J. He and Z. Zhang, *Chem. Eng. J.*, 2021, **405**, 127088.
5 S. Zhang, J. Huang, Y. Cheng, H. Yang, Z. Chen and Y. Lai, *Small*, 2017, **13**.
6 L. Mishchenko, B. Hatton, V. Bahadur, J. A. Taylor, T. Krupenkin and J. Aizenberg, *ACS Nano*, 2010, **4**, 7699–7707.
7 J. Chen, R. Dou, D. Cui, Q. Zhang, Y. Zhang, F. Xu, X. Zhou, J. Wang, Y. Song and L. Jiang, *ACS Appl. Mater. Interfaces*, 2013, **5**, 4026–4030.
8 R. Dou, J. Chen, Y. Zhang, X. Wang, D. Cui, Y. Song, L. Jiang and J. Wang, *ACS Appl. Mater. Interfaces*, 2014, **6**, 6998–7003.
9 H. Yang, C. Ma, K. Li, K. Liu, M. Loznik, R. Teeuwen, J. C. van Hest, X. Zhou, A. Herrmann and J. Wang, *Adv. Mater.*, 2016, **28**, 5008–5012.
10 Z. He, W. J. Xie, Z. Liu, G. Liu, Z. Wang, Y. Q. Gao and J. Wang, *Sci. Adv.*, 2016, **2**, e1600345.
11 J. Chen, Z. Luo, Q. Fan, J. Lv and J. Wang, *Small*, 2014, **10**, 4693–4699.
12 T. Cheng, R. He, Q. Zhang, X. Zhan and F. Chen, *J. Mater. Chem. A*, 2015, **3**, 21637–21646.
13 L. Wang, Q. Gong, S. Zhan, L. Jiang and Y. Zheng, *Adv. Mater.*, 2016, **28**, 7729–7735.
14 X. Gao and L. Jiang, *Nature*, 2004, **432**, 36.
15 M. Liu, S. Wang and L. Jiang, *Nat. Rev. Mater.*, 2017, **2**.
16 T. Maitra, M. K. Tiwari, C. Antonini, P. Schoch, S. Jung, P. Eberle and D. Poulikakos, *Nano Lett.*, 2014, **14**, 172–182.
17 L. Cao, A. K. Jones, V. K. Sikka, J. Wu and D. Gao, *Langmuir*, 2009, **25**, 12444–12448.
18 V. Bahadur, L. Mishchenko, B. Hatton, J. A. Taylor, J. Aizenberg and T. Krupenkin, *Langmuir*, 2011, **27**, 14143–14150.
19 Y. Shen, J. Tao, H. Tao, S. Chen, L. Pan and T. Wang, *Langmuir*, 2015, **31**, 10799–10806.
20 M. Nosonovsky and V. Hejazi, *ACS Nano*, 2012, **6**, 8488–8491.
21 V. Hejazi, K. Sobolev and M. Nosonovsky, *Sci. Rep.*, 2013, **3**, 2194.
22 S. Bengaluru Subramanyam, V. Kondrashov, J. Ruhe and K. K. Varanasi, *ACS Appl. Mater. Interfaces*, 2016, **8**, 12583–12587.
23 A. M. Emelyanenko, L. B. Boinovich, A. A. Bezdomnikov, E. V. Chulkova and K. A. Emelyanenko, *ACS Appl. Mater. Interfaces*, 2017, **9**, 24210–24219.
24 L. B. Boinovich, A. M. Emelyanenko, K. A. Emelyanenko and E. B. Modin, *ACS Nano*, 2019, **13**, 4335–4346.
25 V. Vercillo, S. Tonnicchia, J. M. Romano, A. García-Girón, A. I. Aguilar-Morales, S. Alamri, S. S. Dimov, T. Kunze, A. F. Lasagni and E. Bonaccurso, *Adv. Funct. Mater.*, 2020, 1910268, DOI: 10.1002/adfm.201910268,.

26 V. Vercillo, J. T. Cardoso, D. Huerta-Murillo, S. Tonnicchia, A. Laroche, J. A. Mayén Guillén, J. L. Ocaña, A. F. Lasagni and E. Bonaccurso, *Mater. Lett.: X*, 2019, **3**, 100021.
27 B. Liu, K. Zhang, C. Tao, Y. Zhao, X. Li, K. Zhu and X. Yuan, *RSC Adv.*, 2016, **6**, 70251–70260.
28 G. Momen, R. Jafari and M. Farzaneh, *Appl. Surf. Sci.*, 2015, **349**, 211–218.
29 S. A. Kulinich, S. Farhadi, K. Nose and X. W. Du, *Langmuir*, 2011, **27**, 25–29.
30 T. S. Wong, S. H. Kang, S. K. Tang, E. J. Smythe, B. D. Hatton, A. Grinthal and J. Aizenberg, *Nature*, 2011, **477**, 443–447.
31 Y. Zhuo, F. Wang, S. Xiao, J. He and Z. Zhang, *ACS Omega*, 2018, **3**, 10139–10144.
32 M. J. Coady, M. Wood, G. Q. Wallace, K. E. Nielsen, A. M. Kietzig, F. Lagugne-Labarthet and P. J. Ragogna, *ACS Appl. Mater. Interfaces*, 2018, **10**, 2890–2896.
33 Q. Liu, Y. Yang, M. Huang, Y. Zhou, Y. Liu and X. Liang, *Appl. Surf. Sci.*, 2015, **346**, 68–76.
34 Y. Zhuo, V. Håkonsen, Z. He, S. Xiao, J. He and Z. Zhang, *ACS Appl. Mater. Interfaces*, 2018, **10**, 11972–11978.
35 Y. Zhuo, S. Xiao, V. Håkonsen, T. Li, F. Wang, J. He and Z. Zhang, *Appl. Mater. Today*, 2020, **19**, 100542.
36 Z. He, S. Xiao, H. Gao, J. He and Z. Zhang, *Soft Matter*, 2017, **13**, 6562–6568.
37 Z. He, Y. Zhuo, J. He and Z. Zhang, *Soft Matter*, 2018, **14**, 4846–4851.
38 Y. Zhuo, T. Li, F. Wang, V. Håkonsen, S. Xiao, J. He and Z. Zhang, *Soft Matter*, 2019, **15**, 3607–3611.
39 T. Li, Y. Zhuo, V. Håkonsen, J. He and Z. Zhang, *Ind. Eng. Chem. Res.*, 2019, **58**, 17776–17783.
40 D. L. Beemer, W. Wang and A. K. Kota, *J. Mater. Chem. A*, 2016, **4**, 18253–18258.
41 K. Golovin, S. P. Kobaku, D. H. Lee, E. T. DiLoreto, J. M. Mabry and A. Tuteja, *Sci. Adv.*, 2016, **2**, e1501496.
42 X. Liu, J. Liu, S. Lin and X. Zhao, *Mater. Today*, 2020, DOI: 10.1016/j.mattod.2019.12.026.
43 H. Fan and J. P. Gong, *Macromolecules*, 2020, **53**, 2769–2782.
44 Y. Cao, Y. J. Tan, S. Li, W. W. Lee, H. Guo, Y. Cai, C. Wang and B. C. K. Tee, *Nat. Electron.*, 2019, **2**, 75–82.
45 G. Yang, Y. Song, Q. Wang, L. Zhang and L. Deng, *Mater. Des.*, 2020, **190**, 108563.
46 C. Lu and X. Chen, *Acc. Chem. Res.*, 2020, **53**, 1468–1477.
47 Z. Wang, J. Zhang, J. Liu, S. Hao, H. Song and J. Zhang, *ACS Appl. Mater. Interfaces*, 2021, DOI: 10.1021/acsami.0c21121.
48 Y. Zhuo, S. Xiao, V. Håkonsen, J. He and Z. Zhang, *ACS Mater. Lett.*, 2020, **2**, 616–623.
49 B. Huang, S. Jiang, Y. Diao, X. Liu, W. Liu, J. Chen and H. Yang, *Molecules*, 2020, **25**, 3378.
50 T. Li, P. F. Ibanez-Ibanez, V. Hakonsen, J. Wu, K. Xu, Y. Zhuo, S. Luo, J. He and Z. Zhang, *ACS Appl. Mater. Interfaces*, 2020, **12**, 35572–35578.
51 F. Chen, Z. Xu, H. Wang, S. Handschuh-Wang, B. Wang and X. Zhou, *ACS Appl. Mater. Interfaces*, 2020, **12**, 55501–55509.
52 Y. Ru, R. Fang, Z. Gu, L. Jiang and M. Liu, *Angew. Chem. Int. Ed.*, 2020, **59**, 11876–11880.
53 Q. Guo, Z. He, Y. Jin, S. Zhang, S. Wu, G. Bai, H. Xue, Z. Liu, S. Jin, L. Zhao and J. Wang, *Langmuir*, 2018, **34**, 11986–11991.
54 X. Yao, B. Chen, X. P. Morelle and Z. Suo, *Extreme Mech. Lett.*, 2021, **44**, 101225.
55 S. Nath, S. F. Ahmadi and J. B. Boreyko, *Nanoscale Microscale Thermophys. Eng.*, 2016, **21**, 81–101.
56 N. Miljkovic, R. Enright, Y. Nam, K. Lopez, N. Dou, J. Sack and E. N. Wang, *Nano Lett.*, 2013, **13**, 179–187.
57 Y. Long, X. Yin, P. Mu, Q. Wang, J. Hu and J. Li, *Chem. Eng. J.*, 2020, **401**, 126137.
58 R. P. Sear, *J. Phys.: Condens. Matter*, 2007, **19**, 033101.
59 T. M. Schutzius, S. Jung, T. Maitra, P. Eberle, C. Antonini, C. Stamatopoulos and D. Poulikakos, *Langmuir*, 2015, **31**, 4807–4821.
60 P. Eberle, M. K. Tiwari, T. Maitra and D. Poulikakos, *Nanoscale*, 2014, **6**, 4874–4881.
61 O. R. Enríquez, Á. G. Marín, K. G. Winkels and J. H. Snoeijer, *Phys. Fluids*, 2012, **24**, 091102.
62 G. Graeber, T. M. Schutzius, H. Eghlidi and D. Poulikakos, *Proc. Natl. Acad. Sci. U. S. A.*, 2017, **114**, 11040–11045.
63 S. Jung, M. K. Tiwari and D. Poulikakos, *Proc. Natl. Acad. Sci. U. S. A.*, 2012, **109**, 16073–16078.
64 S. Nath and J. B. Boreyko, *Langmuir*, 2016, **32**, 8350–8365.
65 S. F. Ahmadi, S. Nath, G. J. Iliff, B. R. Srijanto, C. P. Collier, P. Yue and J. B. Boreyko, *ACS Appl. Mater. Interfaces*, 2018, **10**, 32874–32884.
66 Y. Jin, C. Wu, Y. Yang, J. Wu, Z. He and J. Wang, *ACS Nano*, 2020, DOI: 10.1021/acsnano.0c01304.
67 G. Bai, D. Gao, Z. Liu, X. Zhou and J. Wang, *Nature*, 2019, **576**, 437–441.
68 J. Liu, C. Zhu, K. Liu, Y. Jiang, Y. Song, J. S. Francisco, X. C. Zeng and J. Wang, *Proc. Natl. Acad. Sci. U. S. A.*, 2017, **114**, 11285–11290.
69 Y. Jin, Z. He, Q. Guo and J. Wang, *Angew. Chem. Int. Ed. Engl.*, 2017, **56**, 11436–11439.
70 Y. Yao, T. Y. Zhao, C. Machado, E. Feldman, N. A. Patankar and K. C. Park, *Proc. Natl. Acad. Sci. U. S. A.*, 2020, **117**, 6323–6329.
71 Y. Zhao, Z. Yan, H. Zhang, C. Yang and P. Cheng, *Int. J. Heat Mass Transfer*, 2021, **165**, 120609.
72 L. A. Wilen, J. S. Wettlaufer, M. Elbaum and M. Schick, *Phys. Rev. B: Condens. Matter Mater. Phys.*, 1995, **52**, 12426–12433.
73 I. A. Ryzhkin and V. F. Petrenko, *J. Phys. Chem. B*, 1997, **101**, 6267–6270.
74 S. Xiao, J. He and Z. Zhang, *Nanoscale*, 2016, **8**, 14625–14632.
75 S. Xiao, B. H. Skallerud, F. Wang, Z. Zhang and J. He, *Nanoscale*, 2019, **11**, 16262–16269.
76 A. J. Meuler, J. D. Smith, K. K. Varanasi, J. M. Mabry, G. H. McKinley and R. E. Cohen, *ACS Appl. Mater. Interfaces*, 2010, **2**, 3100–3110.
77 Z. He, E. T. Vagenes, C. Delabahan, J. He and Z. Zhang, *Sci. Rep.*, 2017, **7**, 42181.
78 Y. Li, C. Luo, X. Li, K. Zhang, Y. Zhao, K. Zhu and X. Yuan, *Appl. Surf. Sci.*, 2016, **360**, 113–120.

79 P. Juuti, J. Haapanen, C. Stenroos, H. Niemelä-Anttonen, J. Harra, H. Koivuluoto, H. Teisala, J. Lahti, M. Tuominen, J. Kuusipalo, P. Vuoristo and J. M. Mäkelä, *Appl. Phys. Lett.*, 2017, **110**.
80 P. Kim, T. S. Wong, J. Alvarenga, M. J. Kreder, W. E. Adorno-Martinez and J. Aizenberg, *ACS Nano*, 2012, **6**, 6569–6577.
81 H. Yao and H. Gao, *J. Comput. Theor. Nanosci.*, 2010, **7**, 1299–1305.
82 P. Irajizad, A. Al-Bayati, B. Eslami, T. Shafquat, M. Nazari, P. Jafari, V. Kashyap, A. Masoudi, D. Araya and H. Ghasemi, *Mater. Horiz.*, 2019, **6**, 758–766.
83 Y. L. Wang, X. Yao, J. Chen, Z. Y. He, J. Liu, Q. Y. Li, J. J. Wang and L. Jiang, *Sci. China Mater.*, 2015, **58**, 559–565.
84 C. Urata, G. J. Dunderdale, M. W. England and A. Hozumi, *J. Mater. Chem. A*, 2015, **3**, 12626–12630.
85 C. Creton, *Macromolecules*, 2017, **50**, 8297–8316.
86 Y. Wang, X. Yao, S. Wu, Q. Li, J. Lv, J. Wang and L. Jiang, *Adv. Mater.*, 2017, **29**.
87 C. Urata, R. Hönes, T. Sato, H. Kakiuchida, Y. Matsuo and A. Hozumi, *Adv. Mater. Interfaces*, 2019, **6**, 1801358.
88 A. Sandhu, O. J. Walker, A. Nistal, K. L. Choy and A. J. Clancy, *Chem. Commun.*, 2019, **55**, 3215–3218.
89 G. M. Chen, S. C. Liu, Z. Y. Sun, S. F. Wen, T. Feng and Z. F. Yue, *Prog. Org. Coat.*, 2020, **144**, 105641.
90 Y. Yu, B. Jin, M. I. Jamil, D. Cheng, Q. Zhang, X. Zhan and F. Chen, *ACS Appl. Mater. Interfaces*, 2019, **11**, 12838–12845.
91 Y. Jian, S. Handschuh-Wang, J. Zhang, W. Lu, X. Zhou and T. Chen, *Mater. Horiz.*, 2020, DOI: 10.1039/d0mh01029d.
92 M. M. Conde, M. Rovere and P. Gallo, *J. Mol. Liq.*, 2018, **261**, 513–519.
93 S. S. N. Murthy, *Cryobiology*, 1998, **36**, 84–96.
94 T. Chang and G. Zhao, *Adv. Sci.*, 2021, 2002425, DOI: 10.1002/advs.202002425.
95 S. Cerveny, J. Colmenero and A. Alegría, *Macromolecules*, 2005, **38**, 7056–7063.
96 V. Gun'ko, I. Savina and S. Mikhalovsky, *Gels*, 2017, **3**, 37.
97 S. V. Elgersma, M. Ha, J. J. Yang, V. K. Michaelis and L. D. Unsworth, *Materials*, 2019, **12**.
98 Z. He, K. Liu and J. Wang, *Acc. Chem. Res.*, 2018, **51**, 1082–1091.
99 W. Borchard, A. Kenning, A. Kapp and C. Mayer, *Int. J. Biol. Macromol.*, 2005, **35**, 247–256.
100 Z. Wang, B. Lin, S. Sheng, S. Tan, P. Wang, Y. Tao, Z. Liu, Z. He and J. Wang, *CCS Chem.*, 2021, 1–23, DOI: 10.31635/ccschem.021.202000648.
101 P. McConville and J. M. Pope, *Polymer*, 2001, **42**, 3559–3568.
102 M. R. Michaud and D. L. Denlinger, *Int. Congr. Ser.*, 2004, **1275**, 32–46.
103 R. A. Brush, M. Griffith and A. Mlynarz, *Plant Physiol.*, 1994, **104**, 725–735.
104 F. Wang, S. B. Xiao, Y. Z. Zhuo, W. W. Ding, J. Y. He and Z. L. Zhang, *Mater. Horiz.*, 2019, **6**, 2063–2072.
105 Y. Ding, J. Zhang, X. Zhang, Y. Zhou, S. Wang, H. Liu and L. Jiang, *Adv. Mater. Interfaces*, 2015, **2**, 1500177.
106 Y. Cao, T. G. Morrissey, E. Acome, S. I. Allec, B. M. Wong, C. Keplinger and C. Wang, *Adv. Mater.*, 2017, **29**.
107 Y. Liu, A. S. Meyer, Y. Nie, S. Zhang, Y. Zhao, P. L. Fosbøl and K. Thomsen, *J. Chem. Eng. Data*, 2017, **62**, 2374–2383.
108 Y. Huang, L. Xiao, J. Zhou, X. Li, J. Liu and M. Zeng, *J. Mater. Sci.*, 2020, **55**, 14690–14701.
109 B. P. Lee, P. B. Messersmith, J. N. Israelachvili and J. H. Waite, *Annu. Rev. Mater. Res.*, 2011, **41**, 99–132.
110 J. Yang, R. Bai and Z. Suo, *Adv. Mater.*, 2018, **30**, e1800671.
111 W. D. Callister Jr and D. G. Rethwisch, *Fundamentals of materials science and engineering: an integrated approach*, John Wiley & Sons, 2020.
112 Z. Li, Z. Liu, T. Y. Ng and P. Sharma, *Extreme Mech. Lett.*, 2020, **35**, 100617.
113 L. Hu, Y. Wan, Q. Zhang and M. J. Serpe, *Adv. Funct. Mater.*, 2019, **30**, 1903471.
114 J. Li, A. D. Celiz, J. Yang, Q. Yang, I. Wamala, W. Whyte, B. R. Seo, N. V. Vasilyev, J. J. Vlassak, Z. Suo and D. J. Mooney, *Science*, 2017, **357**, 378–381.
115 X. Yao, J. Liu, C. Yang, X. Yang, J. Wei, Y. Xia, X. Gong and Z. Suo, *Adv. Mater.*, 2019, **31**, e1903062.
116 J. Steck, J. Yang and Z. Suo, *ACS Macro Lett.*, 2019, **8**, 754–758.
117 P. Theato, B. S. Sumerlin, R. K. O'Reilly and T. H. Epps, 3rd, *Chem. Soc. Rev.*, 2013, **42**, 7055–7056.
118 X. Yang, Y. Huang, Y. Zhao, X. Zhang, J. Wang, E. E. Sann, K. H. Mon, X. Lou and F. Xia, *Front. Chem.*, 2019, **7**, 826.

